Study of Cold Nuclear Matter effect with prompt D_s meson production in pPb collisions at LHCb

Chenxi Gu

CONTENTS

LIST OF FIGURES

LIST OF TABLES

ABSTRACT

The productions of prompt D_s mesons in proton-lead collisions in the forward and backward configurations are studied. The data are collected with the LHCb detector with $\sqrt{s_{NN}} = 5TeV$(proton beam energy is 4000 GeV,lead beam energy is 1500 GeV). The forward (backward) rapidity range $1.5 < y^* < 3.5(-4.5 < y^* < -2.5)$, the p_T range $0 < p_T < 10GeV/c$. The paper will introduce my work this semaster.

1 INTRODUCTION

Ultra-relativistic heavy-ion collisions are used to study the nuclear matter at high temperature and pressure where the formation of the Quark Gluon Plasma (QGP), a state of matter which consists of asymptotically free quarks and gluons, occurs. Open heavy flavours and quarkonia are produced at the early stages of the collision and might interact with the deconfined medium, making them ideal probes of the QGP. It was indeed predicted that in hot nuclear matter, charmonia are suppressed due to color screening of the heavy quarks potential . Quarkonia can also be suppressed in absence of the QGP formation by Cold Nuclear Matter (CNM) effects. Proton-Nucleus collisions (pA or Ap), which are interesting by themselves, are therefore essential to interpret Nucleus-Nucleus data in order to disentangle QGP effects from CNM effects in those collisions. The main CNM effects affecting quarkonium production include initial-state nuclear effects on the parton densities , the initial-state parton energy loss and final-state energy loss , the final- state absorption of the pre-resonant heavy quark pair by the spectator nucleons albeit small at LHC and the final-state interaction of the quarkonium with the produced medium .

2 LHCB ADVANTAGE IN HEAVY ION PHYSICS

- LHCb is specialised in heavy flavour precision physics, beauty and charm:
  - Optimised for low pile-up collisions(ie low multiplicity):
    - Precise reconstruction of production and decay vertices: time dependent CP violation
    - Correlations between particles: flavour tagging
- Some characteristics of the experiment make it attractive for measurements in Heavy ion physics too:
  - Instruments fully the forward region:$2 < \eta < 5$
  - Precise vertexing:separation of prompt production from B decay products
  - Precise tracking:reconstruction down to $p_T = 0$
  - Particle identification:full reconstruction of hadronic decays of charm or beauty, such as $D_0 \to K\pi$

3 CROSS-SECTION DETERMINATION

The determination of the double-differential production cross-section for prompt D_s requires the knowledge of the numbers of prompt D_s in bins of the kinematic variables4 y^* and p_T, where p_T and y^* are defined in the nucleon-nucleon center-of-mass frame, and the positive z-axis is defined as the direction of the proton beam.

The laboratory frame does not coincide with the center-of-mass frame of the proton-nucleon system, which has a rapidity of $\delta y = \frac{1}{2}\log(A_{Pb}/Z_{Pb}) = 0.465$ in the laboratory frame. Therefore the rapidity in the pN rest frame, y^*, is shifted by a constant value with respect to the rapidity in the laboratory frame, $y = y^* + 0.465$.

Here we define the rapidity with the direction of proton beam as positive z-axis (lead beam as negative z-axis). We thus define the rapidity acceptance in the pN center-of-mass frame to be$1.5 < y^* < 3.5(-4.5 < y^* < -2.5)$for the Fwd(Bwd) collision. For the differential cross-section determination, the bin width for p_T is 1 GeV/c and for y^* 0.5; the signal yields and efficiency are determined separately

for each bin, thanks to the good resolution. The double differential cross-section for prompt D_s production in a given (p_T, y^*) bin is thus defined as:

$$\frac{d^2\sigma}{dp_T dy} = \frac{N(D_s \to K^+K^-\pi)}{L \times \epsilon_{tot} \times B(D_s \to K^+K^-\pi) \times \Delta y \times \Delta p_T} \tag{1}$$

where

- $N(D_s \to K^+K^-\pi)$ is the number of prompt D_s signals reconstructed through the $D_s \to K^+K^-\pi$ decay channel.
- L is the integrated luminosity.
- ϵ_{tot} is the total efficiency determined in each (p_T, y^*) bin
- $B(D_s \to K^+K^-\pi)$ is the branching fraction of the decay $D_s^+ \to K^+K^-\pi^+$ including $D_s^- \to K^+K^-\pi^-$
- $\Delta p_T = 1$ GeV/c is the bin width of the D_s transverse momentum.
- $\Delta y = 0.5$ is the bin width of the D_s rapidity.

The forward and backward cross-section measurements are in the range $p_T(D_s) <$ 10 GeV/c. The rapidity acceptance in the laboratory frame for D_s is roughly $2 < y < 4$ for the Fwd collision, and $-4 < y < -2$ for the Bwd collision.

The total cross-section over a specific range is determined by integrating the double differential cross-section over that particular range. The nuclear modification factor is defined to be the production cross-section in pPb collisions, normalized by the number of nucleons in Pb nucleus , relative to that in pp collisions corresponding to the same nucleon-nucleon center-of-mass energy $\sqrt{s_{NN}}$,

$$R_{pPb} = \frac{1}{A} \frac{\frac{d^2\sigma_{pPb}}{dp_T dy^*}(y^*(p_T), \sqrt{s_{NN}})}{\frac{d^2\sigma_{pp}}{dp_T dy^*}(y^*(p_T), \sqrt{s_{NN}})} \tag{2}$$

studied in bins of p_T and y^* integrated over y^* and p_T respectively. As you can see,R_{pPb} is calculated integrated in all centralities, i.e. averaged over the number of binary proton-nucleon collisions, which is estimated to be around 7 by the ALICE experiment at LHC . Another interesting variable is the forward-backward production ratio for the same absolute rapidity, defined as

$$R_{FB} = \frac{R_{pPb}(+|y^*|(p_T))}{R_{pPb}(-|y^*|(p_T))} \tag{3}$$

also studied in bins of p_T and y^* integrated over y^* and p_T respectively.

4 SIGNAL YIELD DETERMINATION

The signal yield is determined from extended unbinned maximum likelihood fit to the $M(K^+K^-\pi)$ invariant mass distribution.The signal shape is described by a crystal ball function plus a Gaussian. The two components share the mean value μ. In the CB function, we fix $n = 1$ constraint from physics, while a is fixed to 2.72, the value obtained from simulation. The fraction of the CB component is fixed to 0.76. These parameters are also obtained from simulation, and they are found to describe very well the simulation sample in different kinematic bins. The background is described by a linear function. We fit the candidates in the range $M \pm |\Delta M|$ around the observed D_s mass as $M = 1969$ MeV/c2, with $|\Delta M| = 79$ MeV/c2. In Fig. 1, the fitted signal yield in different (p_T, y^*) bins are given. The σ of the CB is known to depend on D_s kinematics while the μ could also be kinematic dependent due

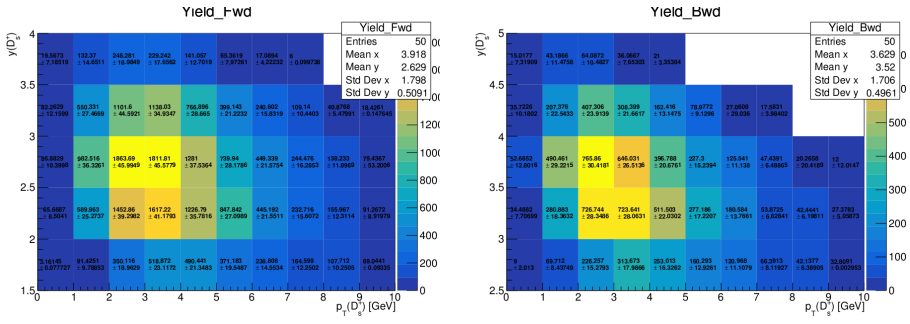

(a) (b)

Figure 1: The fitted total D_s signal yields as a function of p_T and y^* for (left) Fwd and (right) Bwd real data configuration. The empty bins are regions in which the statistics was too low and the fit failed.

to imperfect detector alignment, so in the fit the mean μ and σ are independent parameters in each bin.

To discriminate prompt D_s and D_s from b, the distribution of $\log(\chi^2_{IP}(D_s))$ (10 based logarithm) is fitted to determine the fraction of D_s from b, which is the number of D_s from b candidates over the sum of D_s from b and prompt D_s. The $\log(\chi^2_{IP}(D_s))$ for prompt D_s decays is modelled with a modified gaussian function (f_{AGE}), where the width is allowed to be asymmetric with respect to the mean, and the tails are described by exponential functions

$$f_{AGE}(x;\mu,\sigma,\epsilon,\rho_L,\rho_R) = \begin{cases} e^{\frac{\rho_L^2}{2}+\frac{\rho_L\cdot(x-\mu)}{\sigma\cdot(1-\epsilon)}} & x < \mu-(\sigma\cdot\rho_L\cdot(1-\epsilon)) \\ e^{-(\frac{x-\mu}{\sqrt{2}\sigma\cdot(1-\epsilon)})^2} & \mu-(\sigma\cdot\rho_L\cdot(1-\epsilon)) < x < \mu \\ e^{-(\frac{x-\mu}{\sqrt{2}\sigma\cdot(1+\epsilon)})^2} & \mu < x < \mu+(\sigma\cdot\rho_R\cdot(1+\epsilon)) \\ e^{\frac{\rho_R^2}{2}-\frac{\rho_R\cdot(x-\mu)}{\sigma\cdot(1+\epsilon)}} & x > \mu+(\sigma\cdot\rho_R\cdot(1+\epsilon)) \end{cases} \quad (4)$$

as it was done in previous analyses The tail parameters ρ_L, ρ_R and the asymmetry parameter ϵ are determined from fits to simulated sample.

The $\log(\chi^2_{IP}(D_s))$ distribution for D_s-from-b component is described by a Gaussian function, while the one for combinatorial background is deduced by the S-weight method.

The fitted fractions in different D_s p_T and y^* bins are given in Figs. 2. From the plot we can observe that the fraction lies in the range 0-0.2, and it increases with increasing p_T. It should be noted that these fractions should not be used to extract the production cross section of b-hadrons from that of D_s production. In fact, the two components have very different efficiencies, in particular the lifetime-related selections favors b-hadrons.

The invariant mass and $\log(\chi^2_{IP}(D_s))$ distributions, together with the fits are given in Figs. 3 for two particular kinematic bins, for the Fwd and Bwd sample respectively. Good agreements are found between the mass and $\log(\chi^2_{IP}(D0))$ distributions of signals in data and simulation.

5 NEXT STAGE

Efficiency need to be considered.(Geometrical acceptance efficiency,Reconstruction and selection efficiency & PID efficiency) We can calculate the prompt D_s production, then we can calculate the cross-section,Nuclear modifiction factors & forward-backward ratio.

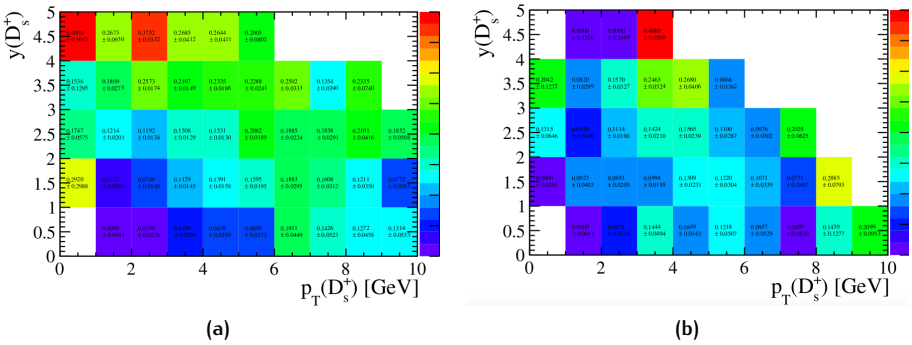

Figure 2: The fitted fractions of D_s-from-b as a function of p_T and y^* for (left) Fwd and (right) Bwd data configuration. Only uncertainties returned by the fit are shown.

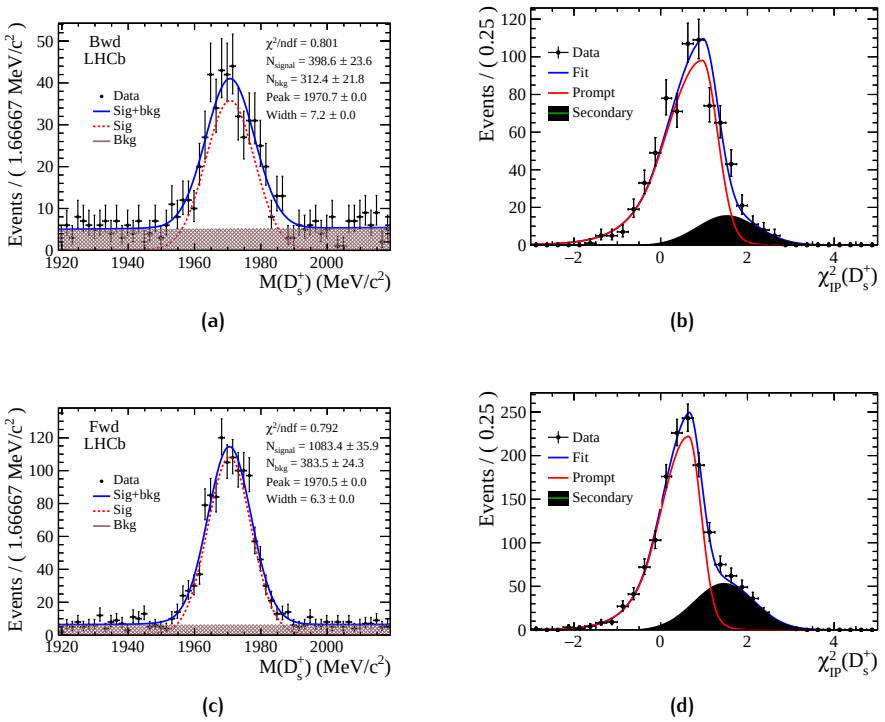

Figure 3: (a) and (b) are $M(D_s)$ and $\chi^2_{IP}(D_s)$ distributions and the fit result for the Bwd, (c) and (d) are $M(D_s)$ and $\chi^2_{IP}(D_s)$ distributions and the fit result for the Fwd